Adsorption Characteristics

DOI: 10.1002/anie.201207908

Metal–Organic Framework Thin Films: Crystallite Orientation Dependent Adsorption**

*Bo Liu, Min Tu, and Roland A. Fischer**

Porous metal–organic frameworks (MOFs) have risen to their fame in material science in the past decades owing to their intrinsic porosities, diversified topologies, and tailored structures and properties, all of which are attractive for a wide spectrum of promising applications for gas storage/separation, greenhouse gas capture, catalysis and sensors, as well as newly established applications in membranes, thin film devices, and biomedical imaging.[1] MOFs as adsorbents, especially for H_2, CO_2, and volatile organic compounds (VOCs, typical hydrocarbons and alcohols, etc.) separation have attracted attention for energy and environmental technologies. Sterics (size/shape exclusion), thermodynamic equilibrium, as well as kinetic and quantum sieving effects are dominant factors in a separation process involving porous materials. Like other kinds of porous materials such as carbon,[2] zeolites,[3] and silica films,[4] MOFs provide interesting potential for selective adsorption and separation at the molecular level because of their pore structures and sizes which can be precisely controlled at the molecular level.[5]

In principle, MOFs crystallized as anisotropic crystallographic systems should exhibit distinct adsorption kinetics for adsorbates approaching from different directions owing to varied pore openings. Nevertheless, most property studies of MOFs have dealt with nanoscale bulky powder or single-crystal samples with randomly distributed crystallite orientations, which exhibits overall adsorption kinetics from all orientations. In contrast, the anisotropic nature of MOF crystals is averaged. One of the very few examples is the anisotropic $[\{Cu_2(bza)_4(pyz)\}_n]$ (bza = benzoate; pyz = pyrazine) as a single-crystal membrane for gas separation, in which the aligned channels gave rise to a much higher permeance and permeation selectivity for H_2 and CO_2 than observed for the nonporous direction.[6] Nevertheless, this study on one single crystal may have limited importance for direct applications since it is challenging to grow large single crystals of MOFs. Advanced thin film/membrane technologies have been coupled with MOFs, and typical examples are ZIF-based membranes.[7] Such membranes displayed superior gas separation performance, and could provide an alternative way of using MOF materials in separation technologies. Although adsorption properties on some well-oriented MOF thin films/membranes have been reported,[8] to the best of our knowledge, no orientation-dependent adsorption on MOF thin films or homogenous ensembles of oriented MOF crystallites attached to surfaces (SURMOFs) has ever been studied.

To investigate anisotropic properties, the first task was to prepare a MOF thin-film material, or better said, a homogeneous sample of MOF crystallites attached to a suitable surface with controlled, uniform orientation. Step-by-step liquid-phase epitaxy (LPE) is suited for this purpose, and involves the oriented growth of MOF nano- and microsized crystallites regulated by the functionality of self-assembled monolayers (SAMs) on substrates.[9] Typically, HKUST-1 coatings with [100] and [111] orientations can be fabricated on carboxylate- and hydroxy-terminated SAMs, respectively, on substrates.[10] Thin films of the jungle-gym structured $[M_2(L)_2(P)]$ (M = Cu^{2+}, Zn^{2+}, Co^{2+}, Ni^{2+}; L = dicarboxylate, P = dinitrogen pillar ligand)[11] were regulated into [100] and [001] orientations by carboxylate- and pyridyl-terminated SAMs, respectively, on substrates.[12a] In this work, we demonstrated the first example of orientation-dependent adsorption behaviors of VOCs using coatings of oriented $[Cu_2(ndc)_2(dabco)]$ (ndc = 1,4-naphthalenedicarboxylate, dabco = 1,4-diazabicyclo[2.2.2]octane) crystallites on a quartz crystal microbalance (QCM) substrate as a model example (Figure 1). The anisotropic $[Cu_2(ndc)_2(dabco)]$ exhibits discriminating pore openings in the [100] and [001] orientations.

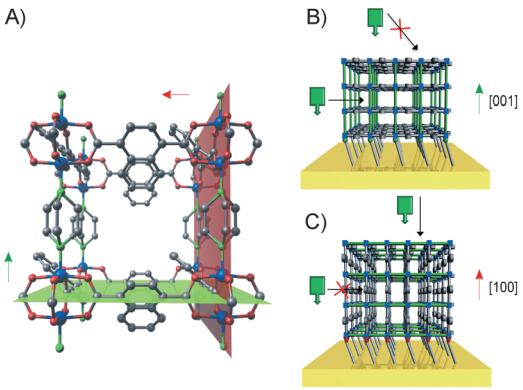

Figure 1. A) Crystallographic structure of $[Cu_2(ndc)_2(dabco)]$, showing the [100] and [001] directions. Schematic illustration of a $[Cu_2(ndc)_2(dabco)]$ thin film fabricated on a PPMT (B) and MHDA (C) SAM having a [001] and [100] orientation, respectively. Their orientation-dependent adsorption behaviors are also depicted.

[*] Dr. B. Liu, M. Sc. M. Tu, Prof. Dr. R. A. Fischer
Chair of Inorganic Chemistry II—Organometallics and Materials Chemistry, Ruhr-Universität Bochum, 44780 Bochum (Germany)
E-mail: roland.fischer@rub.de

[**] This work was funded within the priority program of the German Research Foundation (DFG) on Metal–Organic Frameworks (SPP 1362). B.L. is grateful for a stipend from the Alexander von Humboldt Foundation. M.T. is grateful for a Ph.D. fellowship donated by the China Scholarship Council (CSC).

Supporting information for this article is available on the WWW under http://dx.doi.org/10.1002/anie.201207908.

The layer-based MOF $[Cu_2(ndc)_2(dabco)]$ crystallizes in the tetragonal system containing two faces terminated by copper/ndc (denoted as [001] faces) and four surfaces terminated by copper/dabco (denoted as [100] faces) (Figure 1). Based on the different possible orientations of the ndc linkers in the framework, the pore openings in the [001] and [100] directions were evaluated and range from 7×2 Å^2 to 7×5.7 Å^2 and 2×2 Å^2 to 5.7×5.7 Å^2, respectively. Note, that the dynamic motion of organic linkers plays a role in the control of the adsorption properties (see the Supporting Information).[12b] The latter pore opening is too small to be accessed by most volatile organic compounds (Figure 1). $[Cu_2(ndc)_2(dabco)]$ crystallites oriented in the [001] and [100] directions (denoted as $SURMOF_{001}$ and $SURMOF_{100}$) were fabricated on pyridyl- and carboxylate-terminated SAMs, respectively, on gold-coated QCM substrates using slightly modified procedures which reported by our group previously (see the Experimental Section).[12] The crystallite orientations were confirmed by out-of-plane X-ray diffraction (XRD) with reference to the lattices parallel to the surface, as shown in Figure 2, which also suggested good crystallinity of both

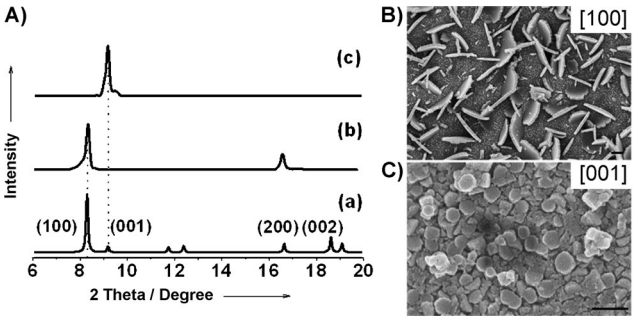

Figure 2. A) Out-of-plane XRD patterns of $[Cu_2(ndc)_2(dabco)]$: a) simulated from powder samples, b) $[Cu_2(ndc)_2(dabco)]$ thin film fabricated on MHDA, and c) PPMT-SAM-functionalized gold (QCM) substrate. SEM images of B) [100] and C) [001] oriented $[Cu_2(ndc)_2(dabco)]$ thin film (scale bar: 400 nm).

samples. Nevertheless, the thin-film morphologies were quite different as observed by SEM (Figure 2). Both samples exhibited similar sheetlike crystallite domains, where $SURMOF_{100}$ sheets stand upright on the substrate and $SURMOF_{001}$ sheets lay down parallel to the surface. SEM images at lower magnification revealed both crystallite coatings are highly homogeneous (see the Supporting Information). For a tetragonal unit cell, the [001] and [100] orientation can be interconverted by a 90° rotation (Figure 1), and is consistent with the observed morphologies between $SURMOF_{100}$ and $SURMOF_{001}$ samples. More surprisingly, $SURMOF_{100}$ crystallites grow separately out of the surface rather than stacking together as do the $SURMOF_{001}$ crystallites, even though the deposition cycles are the same for both samples (40 cycles). This morphology difference can be mainly attributed to the different nucleation and templating effects caused by different functionalities and structural properties of the chosen SAMs on substrates, the effects of which we have discussed previously and a complete understanding of which is still a matter of ongoing research.[12]

The coupling of QCM technology with MOF thin-film research has shown its power in determining diffusion efficiency,[13] surveying the effect of crystal size on sorption kinetics,[14] and investigating the enantioselective adsorption onto enantiopure MOF thin films.[8c] In this work, the $[Cu_2(ndc)_2(dabco)]$ thin film in the both [100] and [001] orientations fabricated on QCM substrates allowed investigation of the orientation-dependent adsorption behaviors, thus taking advantage of the extremely high sensitivity of QCM against mass change. Table 1 summarizes the kinetic

Table 1: VOCs adsorption rates for both $SURMOF_{100}$ and $SURMOF_{001}$ samples.

	Molecular dimensions[15] [Å] at 298 K	Adsorption rate [mg g^{-1} min^{-1}]	
		$SURMOF_{100}$	$SURMOF_{001}$
Benzene (**1**)	5.1×5.8	6.1	1.5
Toluene (**2**)	5.8×6.6	1.1	0.8
p-Xylene (**3**)	6.7×7.4	0.016	0.01

data for the adsorption of volatile organic compounds using both $SURMOF_{100}$ and $SURMOF_{001}$ samples. Benzene, toluene, and xylene were chosen as probe molecules, because they have similar polarities but slightly varied molecular dimensions. $SURMOF_{100}$ exhibited higher adsorption rates for all three compounds when compared to $SURMOF_{001}$. As shown in Figure 1, $SURMOF_{001}$ exposes the crystallographic face comprising two-dimensional Cu/ndc layers to the gas stream. Thus the [001] face actually hinders guest molecules from access because of its comparably small pore opening. However, the larger lateral pore opening derived from a Cu/dabco pillar grid, the [100] face, allows access but is restricted for guest molecules because of the dense lateral stacking of crystallite platelets as evidenced by the SEM image (Figure 2). In contrast, the large pore openings are freely accessible in the $SURMOF_{100}$ sample since they are exposed to the gas stream, and there is no spatial limitation for guest molecules entering because of the much looser lateral stacking of the crystallites in $SURMOF_{100}$ (Figure 2). Impressively, $SURMOF_{100}$ exhibited an initial adsorption rate for benzene that was four times higher than that of $SURMOF_{001}$. With the molecular sizes of adsorbates only slightly increasing, the differentiating effect (denoted as respective adsorption rate in [100]/adsorption rate in [001]) was decreased, with a dramatically decreased absolute adsorption rate. For toluene and *p*-xylene, the differentiating effect is down to 1.4 and 1.6, respectively. The adsorption equilibrium of benzene in both samples was achieved within 6 minutes, which is in contrast to the 40 and 200 min. times needed for toluene and *p*-xylene, respectively (Figure 3). Moreover, in the $SURMOF_{100}$ sample, the initial (kinetic) adsorption selectivity of benzene over toluene and *p*-xylene is 5.5 and 381, respectively, as calculated by the ratio of their apparent initial adsorption rate. These selectivities are much higher

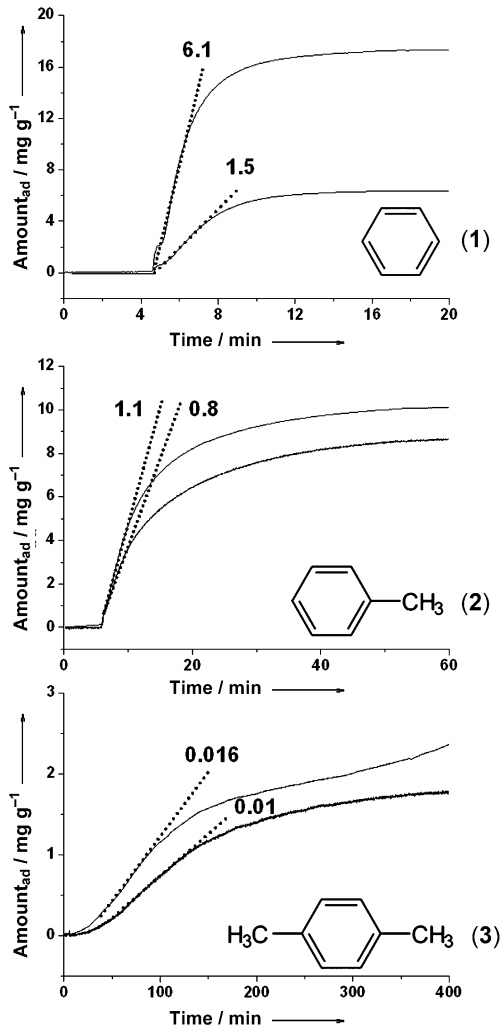

Figure 3. QCM profiles of specific mass uptake of VOCs at the saturated vapor pressure at room temperature for SURMOF$_{001}$ and SURMOF$_{100}$: benzene (**1**), toluene (**2**), and *p*-xylene (**3**). Dotted line represents the adsorption rates (mg g^{-1} min) fitted from the initial linear part of adsorption curves (see also Table 1).

than the corresponding values of 1.8 and 150 determined for the SURMOF$_{001}$ sample. These data demonstrate that the orientation and stacking of the crystallites, which may comprise a MOF thin film, play a major role in their selective adsorption, even though their components and structures are identical.

Ideally, a perfect sample of the [001] oriented [Cu$_2$(ndc)$_2$(dabco)] thin film, which continuously spreads over the whole of the substrate without crystallite boundaries and cracks, will not allow the adsorption of VOCs owing to small pore opening. Similarly, a perfect sample of the [100] oriented [Cu$_2$(ndc)$_2$(dabco)] film will contain densely stacked crystallites which expose their [100] face. Nevertheless, even the orientation as verified by out-of-plane XRD is perfect, and the thin films are comprised of oriented crystallites through either dense or loose stacking (Figure 2). In the case of the dense SURMOF$_{001}$ the boundaries between the laterally stacked plate crystallites obviously provides the passageway for probe molecules entering the larger pore opening from the [100] direction. That is why the adsorption of these VOCs can be observed at all in our SURMOF$_{001}$ samples. Under such circumstances, the saturated adsorption for a certain adsorbate in both types of samples must be the same in theory. Equilibrium adsorption isotherms of benzene, toluene, and *p*-xylene for both SURMOF$_{100}$ and SURMOF$_{001}$ samples were investigated by environment-controlled quartz crystal microbalance (BEL-QCM).[16] The normalized data (see Figure S5 in the Supporting Information) demonstrated that the saturated adsorption amount in both oriented samples are close at different relative humidities, and is consistent with the facts we discussed above.

In summary, we demonstrated the orientation-dependent adsorption behavior of volatile organic compounds for [Cu$_2$(ndc)$_2$(dabco)] thin films in the [100] and [001] orientations. The templating effect of terminal functionality on the substrates supports distinct morphologies for both samples. The results imply that crystallite orientation and stacking of MOF thin films play a significant role in the adsorption properties by controlling guest access to the pores in MOFs. Thin films with crystallites orientated in the [100] direction with a larger pore opening perpendicular to the exposed substrate favored a faster guest molecule uptake and thus points to a higher (kinetic) adsorption selectivity. This work could motivate future investigations with the goal to achieve control of the adsorption/permeation rate in MOFs thin films and membranes through carefully adjusting orientations and morphologies.

Experimental Section

Preparation of SURMOF [Cu$_2$(ndc)$_2$(dabco)]: The PPMT (PPMT = (4-(4-pyridyl)phenyl)methanethiol) and MHDA (MHDA = 16-mercaptohexadecanoic acid) SAMs were fabricated following the procedures described in literature using commercially available quartz crystal microbalance (QCM) Au substrates.[12] The components were applied as diluted ethanol solutions: Cu^{II} acetate hydrate (0.5 mM), an equimolar ndc/dabco mixture (0.2 mM) (ndc = 1,4-naphtalenedicarboxylate; dabco = 1,4-diazabicyclo(2.2.2)octane) as well as ndc (0.2 mM) and dabco (0.2 mM). Typical experiments were carried out using the automated QCM instrument Q-Sense E4 Auto at 40 °C and at flow rates of 100 μL min^{-1}.

Preparation of SURMOF$_{001}$: Each experiment started with exposing the PPMT functionalized QCM substrates first to the Cu^{II} acetate solution for 5 min and then equimolar mixture of linker ndc/dabco for 10 min. Each subsequent step of dosing components was separated by a washing step of 5 min with pure ethanol. Total 40 cycles were applied for SURMOF$_{001}$ growth.

Preparation of SURMOF$_{100}$: Each experiment started with exposing the MHDA functionalized QCM substrates first to the Cu^{II} acetate solution for 5 min and then ndc solution for 10 min, followed by dabco solution for another 10 min. Each subsequent step of dosing components was separated by a washing step of 5 min with pure ethanol. Total 40 cycles were applied for SURMOF$_{100}$ growth.

VOCs adsorption by QCM: Typically, SURMOF (40 cycles) samples (in both [001] and [100] orientation) fabricated on QCM gold substrate were applied. Prior to the VOCs adsorption, SURMOF samples on QCM substrate were evacuated by flowing nitrogen gas overnight at 40 °C to remove accommodated guest molecules. Before switching to vessel containing VOCs, pure nitrogen gas (carrier gas) was flowed over SURMOF sample to obtain stable baseline. Evacuated samples were exposed to the atmosphere of VOC at its naturally generated pressure at a flow rate of 20 mL min^{-1} of carrier

gas (nitrogen gas) controlled by a flow meter and at room temperature.

VOCs adsorption isotherms were measured by an environment controlled quartz crystal microbalance set-up (BEL-Japan). More details are described in Ref. [16].

Received: October 1, 2012
Revised: November 30, 2012
Published online: February 12, 2013

Keywords: adsorption · copper · metal–organic frameworks · structure elucidation · thin films

[1] a) J.-R. Li, J. Sculley, H.-C. Zhou, *Chem. Rev.* **2012**, *112*, 869 – 932; b) M. P. Suh, H. J. Park, T. K. Prasad, D.-W. Lim, *Chem. Rev.* **2012**, *112*, 782 – 835; c) K. Sumida, D. L. Rogow, J. A. Mason, T. M. McDonald, E. D. Bloch, Z. R. Herm, T.-H. Bae, J. R. Long, *Chem. Rev.* **2012**, *112*, 724 – 781; d) A. Corma, H. García, F. X. Llabrés i Xamena, *Chem. Rev.* **2010**, *110*, 4606 – 4655; e) A. Bétard, R. A. Fischer, *Chem. Rev.* **2012**, *112*, 1055 – 1083; f) L. E. Kreno, K. Leong, O. K. Farha, M. Allendorf, R. P. Van Duyne, J. T. Hupp, *Chem. Rev.* **2012**, *112*, 1105 – 1125; g) P. Horcajada, R. Gref, T. Baati, P. K. Allan, G. Maurin, P. Couvreur, G. Férey, R. E. Morris, C. Serre, *Chem. Rev.* **2012**, *112*, 1232 – 1268.

[2] M. B. Shiflett, H. C. Foley, *Science* **1999**, *285*, 1902 – 1905.

[3] Z. Lai, G. Bonilla, I. Diaz, J. G. Nery, K. Sujaoti, M. A. Amat, E. Kokkoli, O. Terasaki, R. W. Thompson, M. Tsapatsis, D. G. Vlachos, *Science* **2003**, *285*, 456 – 460.

[4] R. M. de Vos, H. Verweij, *Science* **1998**, *279*, 1710 – 1711.

[5] J.-R. Li, R. J. Kuppler, H.-C. Zhou, *Chem. Soc. Rev.* **2009**, *38*, 1477 – 1504.

[6] S. Takamizawa, Y. Takasaki, R. Miyake, *J. Am. Chem. Soc.* **2010**, *132*, 2862 – 2863.

[7] a) H. Bux, F. Liang, Y. Li, J. Cravillon, M. Wiebcke, J. Caro, *J. Am. Chem. Soc.* **2009**, *131*, 16000 – 16001; b) Y.-S. Li, F.-Y. Liang, H. Bux, A. Feldhoff, W.-S. Yang, J. Caro, *Angew. Chem.* **2010**, *122*, 558 – 561; *Angew. Chem. Int. Ed.* **2010**, *49*, 548 – 551; c) Y.-S. Li, H. Bux, A. Feldhoff, G.-L. Li, W.-S. Yang, J. Caro, *Adv. Mater.* **2010**, *22*, 3322 – 3326; d) A. Huang, H. Bux, F. Steinbach, J. Caro, *Angew. Chem.* **2010**, *122*, 5078 – 5081; *Angew. Chem. Int. Ed.* **2010**, *49*, 4958 – 4961; e) A. Huang, W. Dou, J. Caro, *J. Am. Chem. Soc.* **2010**, *132*, 15562 – 15564.

[8] a) H. Bux, A. Feldhoff, J. Cravillon, M. Wiebcke, Y.-S. Li, J. Caro, *Chem. Mater.* **2011**, *23*, 2262 – 2269; b) C. Scherb, R. Koehn, T. Bein, *J. Mater. Chem.* **2010**, *20*, 3046 – 3051; c) B. Liu, O. Shekhah, H. K. Arslan, J. Liu, C. Wöll, R. A. Fischer, *Angew. Chem.* **2012**, *124*, 831 – 835; *Angew. Chem. Int. Ed.* **2012**, *51*, 807 – 810.

[9] a) B. Liu, R. A. Fischer, *Sci. China Chem.* **2011**, *54*, 1851 – 1866; b) D. Zacher, O. Shekhah, C. Woll, R. A. Fischer, *Chem. Soc. Rev.* **2009**, *38*, 1418 – 1429.

[10] O. Shekhah, H. Wang, D. Zacher, R. A. Fischer, C. Wöll, *Angew. Chem.* **2009**, *121*, 5138 – 5142; *Angew. Chem. Int. Ed.* **2009**, *48*, 5038 – 5041.

[11] a) D. N. Dybtsev, H. Chun, K. Kim, *Angew. Chem.* **2004**, *116*, 5143 – 5146; *Angew. Chem. Int. Ed.* **2004**, *43*, 5033 – 5036; b) H. Chun, D. N. Dybtsev, H. Kim, K. Kim, *Chem. Eur. J.* **2005**, *11*, 3521 – 3529; c) D. Tanaka, M. Higuchi, K. Hasegawa, S. Horike, R. Matsuda, Y. Kinoshita, N. Yanai, S. Kitagawa, *Chem. Asian J.* **2008**, *3*, 1343 – 1349; d) T. Uemura, Y. Ono, K. Kitagawa, S. Kitagawa, *Macromolecules* **2008**, *41*, 87 – 94; e) H. Wang, J. Getzschmann, I. Senkovska, S. Kaskel, *Microporous Mesoporous Mater.* **2008**, *116*, 653 – 657; f) P. Song, Y. Li, B. He, J. Yang, J. Zheng, X. Li, *Microporous Mesoporous Mater.* **2011**, *142*, 208 – 213.

[12] a) D. Zacher, K. Yusenko, A. Bétard, S. Henke, M. Molon, T. Ladnorg, O. Shekhah, B. Schüpbach, T. de Los Arcos, M. Krasnopolski, M. Meilikhov, J. Winter, A. Terfort, C. Wöll, R. A. Fischer, *Chem. Eur. J.* **2011**, *17*, 1448 – 1455; b) S. Horike, R. Matsuda, D. Tanaka, S. Matsubara, M. Mizuno, K. Endo, S. Kitagawa, *Angew. Chem.* **2006**, *118*, 7384 – 7388; *Angew. Chem. Int. Ed.* **2006**, *45*, 7226 – 7230.

[13] O. Zybaylo, O. Shekhah, H. Wang, M. Tafipolsky, R. Schmid, D. Johannsmann, C. Wöll, *Phys. Chem. Chem. Phys.* **2010**, *12*, 8092 – 8097.

[14] H. Uehara, S. Diring, S. Furukawa, Z. Kalay, M. Tsotsalas, M. Nakahama, K. Hirai, M. Kondo, O. Sakata, S. Kitagawa, *J. Am. Chem. Soc.* **2011**, *133*, 11932 – 11935.

[15] H. Wu, Q. Gong, D. H. Olson, J. Li, *Chem. Rev.* **2012**, *112*, 836 – 868.

[16] A. Bétard, S. Wannapaiboon, R. A. Fischer, *Chem. Commun.* **2012**, *48*, 10493 – 10495.

